

Improvement of DSOGI PLL Synchronization Algorithm with Filter on Three-Phase Grid-Connected Photovoltaic System

Rofiatul Izah *, Subiyanto, Dhidik Prastiyanto

*Electrical Engineering Department
Universitas Negeri Semarang
Office E11 Sekaran Campus 50229
Semarang, Indonesia*

Abstract

Synchronous Reference Frame Phase Locked Loop (SRF PLL) has been widely used for synchronization three-phase grid-connected photovoltaic (PV) system. On the grid fault, SRF PLL distorted by negative sequence component and grid harmonic that caused an error in estimating parameter because of ripple and oscillation. This work combined SRF PLL with Dual Second Order Generalized Integrator (DSOGI) and filter to minimize ripple and minimize oscillation in the phase estimation and frequency estimation. DSOGI was used for filtering and obtaining the 90° shifted versions from the $v_{\alpha\beta}$ signals. These signals ($v_{\alpha\beta}$) were generated from three phase grid voltage signal using Clarke transform. The $v_{\alpha\beta}$ signal was the inputs to the positive-sequence calculator (PSC). The positive-sequence $v_{\alpha\beta}$ was transformed to the dq synchronous reference frame and became an input to SRF-PLL to create the estimation frequency. This estimation frequency from SRF PLL was filtered by the low-pass filter to decrease grid harmonic. Moreover, the output of low-pass filter was a frequency adaptive. The performance of DSOGI PLL with filter is compared with DSOGI PLL, SRF PLL, and IEEE standard 1547(TM)-2003. The improvement of DSOGI PLL with filter gave better performances than DSOGI PLL and SRF PLL because it minimized ripples and oscillations in the phase and frequency estimations.

Keywords: synchronization, DSOGI PLL, PSIM, photovoltaic system, grid connected.

I. INTRODUCTION

Several countries in the world developed renewable energy systems. They are used to reduce environmental damage. One of the most potentials of Renewable Energy Source (RES) is photovoltaic (PV) [1]–[3].

The Distributed Generation (DG) system enables interconnecting RES with grid [4]. One of the alternatives to support the available traditional energy sources in meeting the demand for power by customers is grid-connected PV system [5]. Grid-connected PV system must obey international standards for interconnecting RES with electric power systems [6].

The three-phase PV system injects active and reactive power into the grid using a control power conditioning system (PCS) [7]. PCS is also handling conditions of grid fault [8]. PV produces DC voltage so PCS in PV system consists of the chopper circuit and grid side converter (GSC). Chopper circuit function as DC power controller such as boost converter while GSC such as the inverter is used to convert DC voltage into AC voltage [9].

Synchronization manages interconnection grid-connected PV system by synchronizing the output of inverter with grid specifications. The input of the synchronization is three phase grid voltage signal [10], while the output of the synchronization is amplitude,

phase angle, and frequency estimation [11], [12]. The classic method SRF PLL is called *dq* PLL or park transform based PLL because this method is required for park transformation. SRF PLL is the most commonly used for synchronization [11]. In the synchronization process, the SRF PLL is known as PLL, that is simple and easy to be implemented in the system. This method requires orthogonal voltage system to estimate the phase angle, frequency, and amplitude of the grid voltage [10]–[12].

Second order generalized integrator (SOGI) has several functions such as filter, phase shifted reference waveforms regulator, and signal parameters estimation such as amplitude, frequency, and phase angle [13], [14]. SOGI is used to generate an orthogonal voltage system as an input of PLL to estimate signal parameter [14]. In the three-phase system, Dual second order generalized integrator (DSOGI) is used to estimate signal parameter [13], [15], [16].

Unbalance grid conditions disturb the interconnecting in SRF PLL [17]. Mostly, SRF PLL in single phase is distorted by negative sequence component [18]. SRF PLL which is distorted by negative sequence component caused by unbalance grid conditions creates some errors on phase estimation by oscillation [19]. During grid voltage amplitude variations, and frequency variations, SRF PLL on single phase takes a long time to reach the settling time [20]. SRF PLL is sensitive to the unbalance grid conditions and the frequency variations, influenced frequency and phase estimations [21]. In [17]–[21] SRF PLL is

* Corresponding Author.

Email: izahrofiatul@students.unnes.ac.id

Received: January, 09 2018 ; Revised: February, 28 2018

Accepted: April, 12 2018 ; Published: August, 31 2018

© 2018 PPET - LIPI

combined with SOGI to handle the problem caused by grid conditions. This combination increases harmonic ripple when frequency adaptive experiences deviations of second harmonic ripples. In the three-phase grid-connected PV system, the unbalance grid conditions and the grid harmonic distortions, frequency and phase estimations of SRF PLL are distorted by negative sequence component and harmonic.

In this paper, DSOGI-PLL synchronization algorithm with filter is used to remove the negative-sequence component and filter the harmonic distortion. The phase angle estimation, frequency estimation, THD current (THDi), and power flow condition are obtained from simulated DSOGI PLL synchronization algorithm with filter. The DSOGI PLL synchronization algorithm with filter is compared with DSOGI PLL, SRF PLL and IEEE standard 1547 (TM)-2003 [22]. The result of simulation shows that the DSOGI PLL with filter reduces the oscillation and harmonic ripple on estimation phase and estimation frequency.

Section 2 will describe the three-phase grid-connected PV system. SRF PLL synchronization algorithm is described in Section 3. The main section is DSOGI PLL synchronization algorithm with filter on three-phase grid-connected PV systems is included in Section 4. Simulation of synchronization on three-phase grid-connected PV system using software PSIM is described in section 5. Section 6 will present the results and analysis of the simulation DSOGI PLL synchronization algorithm with filter on three-phase grid-connected PV system. Section 7 of this paper contains the conclusions of this paper.

II. GRID-CONNECTED PHOTOVOLTAIC SYSTEM

The grid-connected PV system requires an observer of the power flow from the renewable energy source to grid [23]. PCS use to control the power factor on the Voltage Source Inverter (VSI) as well as ensure the power quality which is injected into the grid [8], [23].

Block diagram of three-phase grid-connected PV system shows in Figure 1 [11], [24].

The global three-phase grid-connected PV system consists of two subsystems that are power subsystems, and the control subsystems [25]. Power subsystem consists of PV panels, boost converter, VSI, and filter L. PV panels produce DC power according to the level of illumination and temperature [26], [27]. The series-parallel arrangement of PV panels is also affect the power produced by PV [28]. VSI is composed of semiconductor electronic devices such as diodes and IGBTs [29]. VSI is used to convert DC power into AC power [30]. While the PWM works as controller of IGBT on VSI by giving the signal as the power to switch [31]. Figure 1 shows the power of PV on the DC side of the inverter which is described in (1), (2) and (3) [25].

$$i_{boost} = i_{clink} - i_{cc} \quad (1)$$

$$i_{cc} = s_a i_a + s_b i_b + s_c i_c \quad (2)$$

$$i_{clink} = c_{dc} \frac{dv_{boost}}{dt} \quad (3)$$

where i_{boost} , v_{boost} is the current and output voltage boost converter, i_{cc} is the current flows into the three-phases of VSI, i_{clink} is current to the capacitor, c_{clink} is the value of the capacitor, V_{dc} is the voltage across the capacitor, s_a , s_b , s_c is the state of the power-poles (1: 'on', 0: 'off', and s_a , s_b , s_c is upper pole, s_a' , s_b' , s_c' is lower pole in the 3-phase VSI), and the line currents are i_a , i_b , i_c .

The power flow from the three-phase VSI uses the theory of active power (p) and reactive power (q). Active power (p) and reactive power (q) can be expressed in (4), (5) [25], [24].

$$p = v_{sa} \times i_a + v_{sb} \times i_b + v_{sc} \times i_c \quad (4)$$

$$q = \frac{1}{\sqrt{3}} \{ (v_{sa} - v_{sb}) \times i_a + (v_{sb} - v_{sc}) \times i_b + (v_{sc} - v_{sa}) \times i_c \} \quad (5)$$

where v_{sa} , v_{sb} , v_{sc} is the voltage system and i_a , i_b , i_c is the current in the system.

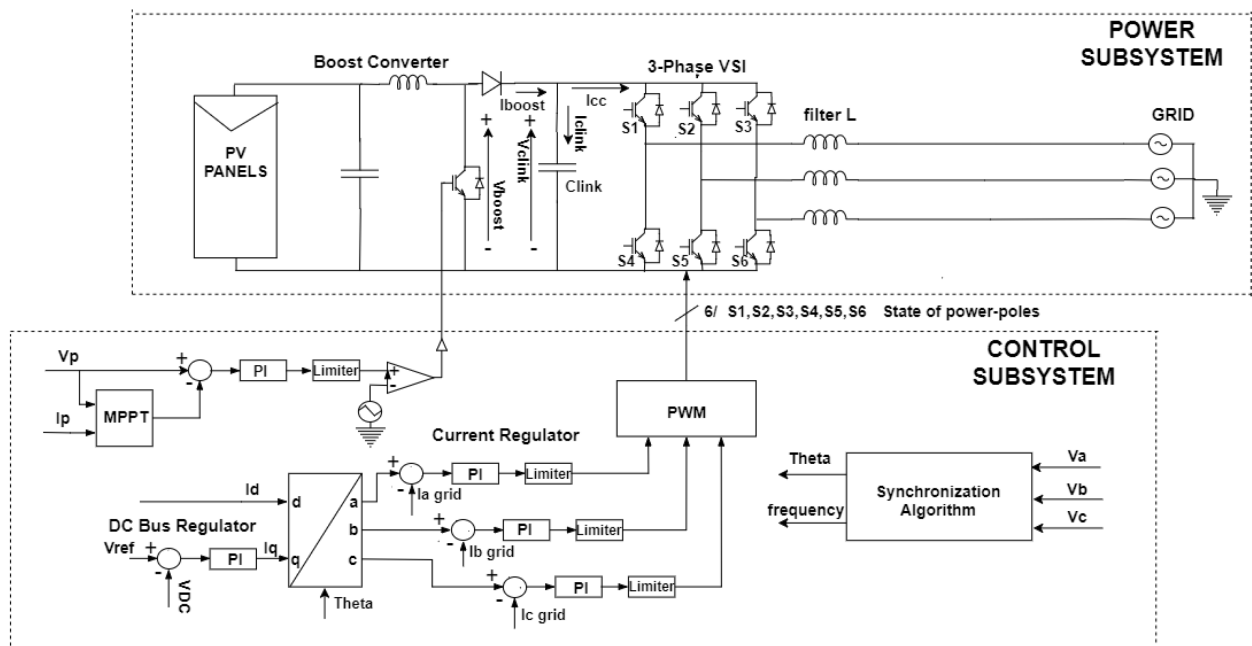


Figure 1. Block diagram of three-phase grid-connected photovoltaic system.

Beside regulating the power flow, PV power system ensures the power quality by obeying the power quality regulation where the total THD current and THD voltage in the three-phase system is 5%, and follow some other rules [22]. The standard resume for RES connections with a grid is explained on [6]. The control subsystem consists of the Maximum Power Point Tracking (MPPT) algorithm, the outer loop PI controller, the inner loop PI controller and the synchronization algorithm [24]. MPPT is one of the important algorithms for grid-connected PV system, for tracking the maximum power of PV Panels [32].

At the outer loop, the DC voltage regulator on the capacitor link is compared to the DC voltage reference of the MPPT control. It aims to keep the DC voltage on the DC side of the inverter to be constant and ensures the power flow between the PV source and the utility grid. The output of outer loop is an input of the PI controller inner loop according to [24] to generate iq^* on the dq reference frame. While id^* is obtained from open loop control power factor.

III. SRF PLL ALGORITHM SYNCHRONIZATION

SRF PLL synchronization Algorithm is widely used in the synchronization three-phase grid-connected PV system. The primary arrangement of SRF PLL is shown in Figure 2 and it includes 3 basic blocks [33].

Figure 2 shows SRF PLL synchronization algorithm consist of three basic blocks, the first block is phase detector in the SRF PLL using park transform. This block is used to generate the difference of phase between the input signal and the output signal. The second is loop filter used as filtering features to eliminate the high-frequency from the Phase Detector output. Usually, the second block consists of PI controller or first-order low-pass filter. The third block is voltage controlled oscillator (VCO). In this block, the angular frequency of grid voltage is added to generate the frequency and phase estimation. The equation of phase estimation and frequency estimation from SRF PLL are calculated using (6) and (7) [33].

$$\omega'(s) = \frac{(k_p + k_i \cdot T_s)s - k_p}{s-1} \cdot v_q^+(s) + \omega \quad (6)$$

$$\theta' = \frac{T_s \cdot s}{s-1} \cdot \omega'(s) \quad (7)$$

where k_i and k_p are parameters on PI, T_s is the sampling time of the continuous system, ω is the angular frequency of grid voltage, v_q^+ is an input signal from a grid, ω' is frequency estimation and θ' is phase estimation.

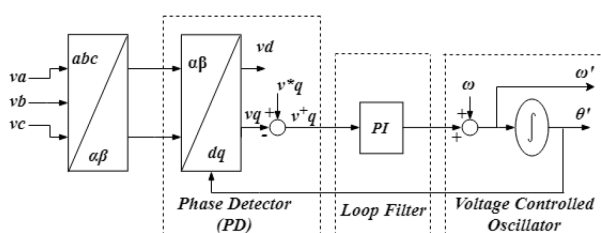


Figure 2. Block diagram of SRF PLL for Three Phase

IV. DSOGI PLL SYNCHRONIZATION ALGORITHM WITH FILTER

A synchronization algorithm is required to obtain a controllable power factor from the grid voltage signal [23]. However, the voltage signal can be distorted by the unbalance grid condition. In addition, the error of the sensor can produce second-order harmonic [34]. On the three-phase utility grid, Positive Sequence Detector (PSD) based on the symmetrical component method or Fortescue theorem on [35] is used on Dual Second Order Generalized Integrator Phase Locked Loop (DSOGI PLL) synchronization algorithm [16], [36], [37]. Generally, DSOGI PLL is developed using grid voltage signal on the stationary reference frame (α, β) . Quadrature signals generated based on double SOGI (QSG) are used to filter and obtain quadrature signals, the signals that shift 90° from the original signal. The transfer function of SOGI is explained by (8) and the block diagram of a quadrature signal based on SOGI (QSG) is presented in Figure 3 [34], [36], where ω' is the frequency adaptive and k is the gain of the SOGI (QSG). Then the signal obtained from DSOGI quadrature signals generator (QSG) is used as inputs on the instantaneous symmetrical components (ISC) method in the stationary reference frame $(\alpha\beta)$. This voltage on stationary reference frame will be transformed into dq form and will be used by SRF PLL to make adaptive frequency and phase angle estimation.

$$SOGI(s) = \frac{v'}{k_{ev}}(s) = \frac{\omega's}{s^2 + \omega'^2} \quad (8)$$

From the Figure 3, the transfer functions of the in-quadrature signals respectively suggest a behavior of band-pass filter $D(s)$ and low-pass filter $Q(s)$. The transfer functions of the filters are described by (9) and (10) [34], [36].

$$D(s) = \frac{v'}{v}(s) = \frac{k\omega's}{s^2 + k\omega's + \omega'^2} \quad (9)$$

$$Q(s) = \frac{qv'}{v}(s) = \frac{k\omega'^2}{s^2 + k\omega's + \omega'^2} \quad (10)$$

Equation (10) implies a lag of 90° between qv' and v , and is not a function of the variation of ω' and k . This function is insensitive to the frequency variations in the input signal (v) when $\omega = \omega'$ (ω is the angular frequency of the input signal). Equations (9) and (10) are second order transfer functions. Their dynamic response will depend on the localization of the poles in the complex plane. In addition, the behavior of the band-pass and low-pass filter described above suggest the harmonic rejection capability of this system.

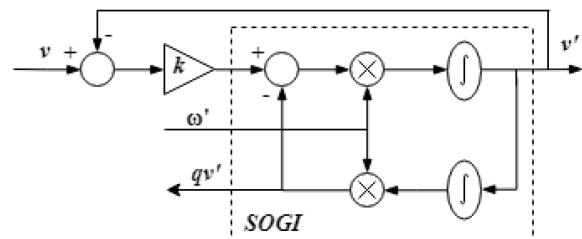


Figure 3. Block diagram of a Second Order Generalized Integrator.

The precise setting of this system of k on a specific ω' makes a trade-off between the proper bandwidth for harmonic rejection and the proper settling time with the corresponding overshoot for the dynamic response.

Table 1 resumes the influence of gain (k) in the SOGI-QSG behavior according to the settling time, overshoot, damping factor, and harmonic rejection of $Q(s)$. When the value of the gain k is higher, the settling time will give better performance and faster response. The transient response has the biggest overshoot and undershoot but the immunity to the harmonics decreases and obtain a bad transient response. When the value of the gain k is lower, the transient response of the SOGI to achieve on settling time becomes longer, but the immunity response of the harmonics is good and obtain better transient response. The gain k setting on 1.414 [34], [35] is a good trade-off between the harmonic rejection (for 5th and 7th harmonics) and the dynamic response is achieved, corresponding to a damping factor $\zeta_{\text{SOGI-QSG}} = 0.707$ for second order systems [34].

Refer to (6), (7) and (8), ω' is the estimated frequency and k is the gain factor of SOGI-QSG. Filter bandwidth is exclusively determined by the gain value and independent of frequency estimation. Time response of SOGI-QSG is described in (11) [34]. The gain factor value of SOGI QSG (k) is presented in Table 1.

$$t_s(\text{SOGI}) = \frac{10}{k\omega'} \quad (11)$$

The DSOGI PLL synchronization algorithm with filter can be analyzed more extensively on a three-phase system as shown in Figure 4. Clarke transformation [38] is applied to transform voltage signal from the grid to be voltage components (α, β). Dual SOGI-QSG is used to obtain the quadrature signal. The positive sequence component generated by Positive Sequence Calculator (PSC) based on ISC as described in (12) $q = e^{-j(\pi/2)}$ is a 90° lagging phase-shift operator applied on the time domain to obtain an in-quadrature version of an input waveform [35].

TABLE I
SOGI QSG BEHAVIOR ACCORDING TO GAIN

k	$\zeta_{\text{SOGI-QSG}}$	Overshoot (%)	Settling time (ms)	Harmonic rejection of $Q(s)$ [dB]	
				5 th	7 th
1	1	0	29.3	-27.72	-33.7
1.25	0.8	1.5	23.4	-25.89	-31.81
1.414	0.707	4.3	20.7	-24.9	-30.78
2	0.5	16.3	14.6	-22.23	-27.94

The bold is the optimal value of k .

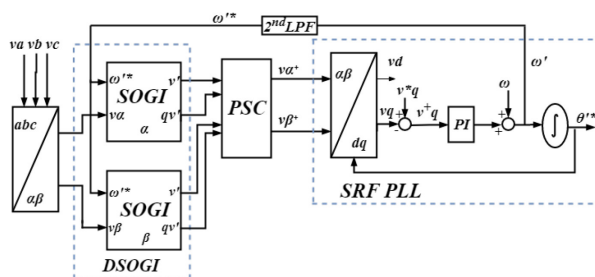


Figure 4. Block diagram of DSOGI PLL

$$\begin{bmatrix} v_{\alpha}^+ \\ v_{\beta}^+ \end{bmatrix} = \frac{1}{2} \begin{bmatrix} 1 & -q \\ q & 1 \end{bmatrix} \begin{bmatrix} v_{\alpha} \\ v_{\beta} \end{bmatrix} \quad (12)$$

The PSC must be designed and applied to the quadrature output signal to calculate the positive sequence components of the unbalanced three-phase grid voltage. Finally, the phase angle and frequency estimation is acquired by using SRF PLL [15], and can be calculated by (13) and (14).

$$\omega'(s) = \frac{(k_p + k_i \cdot T_s)s - k_p}{s-1} \cdot v_q^+(s) + \omega \quad (13)$$

$$\theta' = \frac{T_s \cdot s}{s-1} \cdot \omega'(s) \quad (14)$$

where k_i , k_p is a constant PI, T_s is the sampling time of the continuous system, ω is frequency nominal, ω' is frequency estimation, θ' is phase estimation, and v_q^+ is an output of park transformation and an input of SRF PLL as well.

The estimation frequency of SRF PLL to make the adaptive frequency can be distorted by second order harmonic that produces the harmonic in the other order. Second order LPF is used to filter the second order harmonic on the estimation frequency and make the frequency adaptive better than before using 2nd LPF. The transfer function of 2nd LPF is described on (15).

$$\omega'^* = \frac{k_f \omega'}{s^2 + 2\zeta \omega' s + \omega'^2} \quad (15)$$

where k_f is gain of the filter, ζ is damping ratio, ω' is angular frequency, and f_c is cut off frequency, in Hz $f_c = (\omega'/2\pi)$.

V. SIMULATION OF SYNCHRONIZATION ON THREE-PHASE GRID-CONNECTED PV SYSTEM

Some simulations have been performed using the Power Simulation (PSIM) version 9.0.3 to evaluate the synchronization algorithm. Figure 5 shows simulation model of the three-phase grid-connected PV system. The specification used on this Simulink is JA PV, with output power system 15,000 W in standard conditions (1000 W/m² and 25° C). Parameters used in this system are based on a three-phase inverter built with the 6 IGBTs semiconductors for the three-phase power-poles and configured to work at 15000 KHz of PWM switching frequency. The linear load is a load with the constant sine wave. The linear load sources are incandescent lamps, heaters etc. In this simulation, the linear load used is resistor. The Non-linear load is a load that is not a constant sine wave, where the sine wave distorted with another sine wave. The non-linear load source are a rectifier, motor, computer, switched-mode power supplies, etc. In this simulation the non-linear load used is a three-phase full bridge rectifier [39], [40].

Table 2 contains the value of the components of the L filter, the utility grid, and the values of the parameters for the control subsystem including the parameter of SRF PLL, DSOGI PLL, and DSOGI PLL with filter. The PI parameter in this work is generated by trial and error [41].

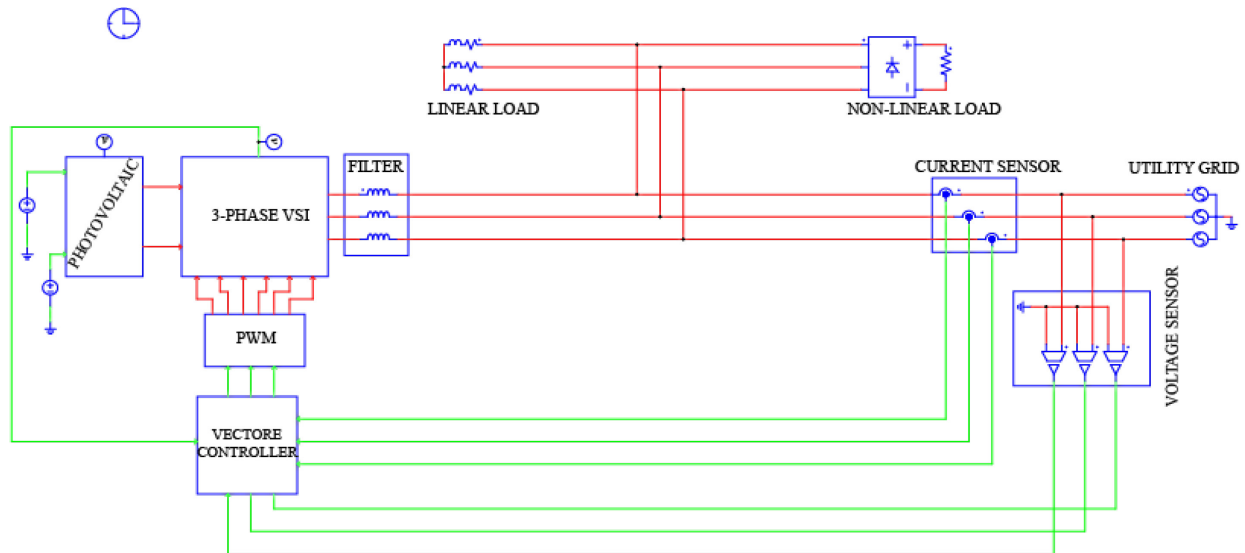


Figure 5. Simulink model of three-phase grid-connected photovoltaic system on PSIM.

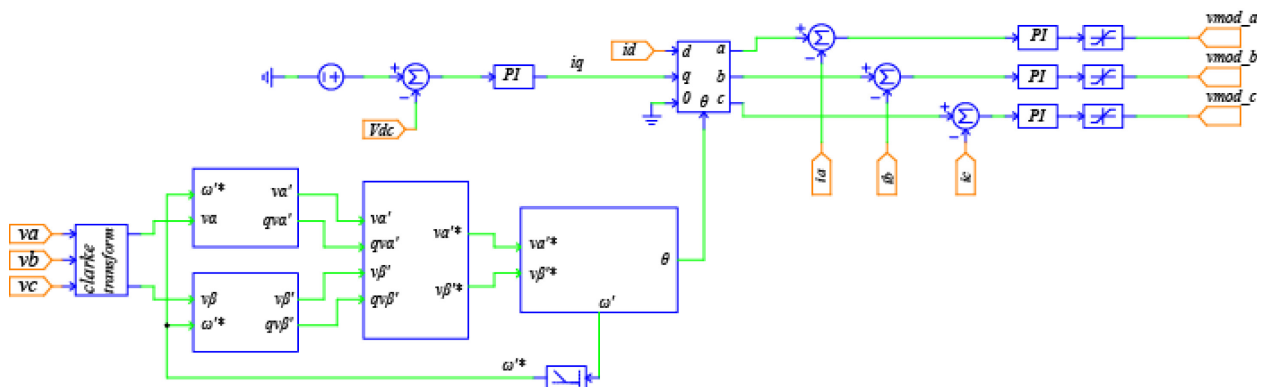


Figure 6. Simulink model of synchronization, current control, and DC link control.

 TABLE 2
 PARAMETER OF POWER SUBSYSTEM AND CONTROL SUBSYSTEM.

3-phase utility grid	= v_{rms} 380 V Frequency 50 Hz
L filter	= 4.05 m
C boost	= 2.35 m
L boost	= 0.188 m
V_{dc}	= 750 Volt
C_{link}	= 0.173 m
F_{cl}	= 15.000 Hz
k_i inner control loop	= 1000
k_i outer control loop	= 1000
Ω	= 3.14
F_{cv}	= 15.000 Hz
k_i of SRF PLL	= 1000
k_p of SRF PLL	= 1000
K of DSOGI PLL and DSOGI PLL with Filter	= 1.414
k_i of DSOGI PLL and DSOGI PLL with Filter	= 0.17725
k_p of DSOGI PLL and DSOGI PLL with Filter	= 0.167954

Figure 6 shows The Simulink of the DSOGI PLL synchronization algorithm with filter and cascade control included in the vector controller block. The

cascade control consists of the outer loop regulator to get the comparison of dc bus voltage in the link capacitor and the reference which comes from the MPPT algorithm. This control loop has been performed using PI controllers. The three PI controllers used in the inner control loop are used to regulate a , b , c components of the line currents (i_a , i_b , i_c).

VI. RESULT AND DISCUSSION

In this section, the performance of DSOGI PLL synchronization algorithm with filter is evaluated on dynamic and transient response under various conditions. The performance of DSOGI PLL with filter is also evaluated on linear load and non-linear load. Performance of DSOGI PLL with filter is compared with DSOGI PLL and SRF PLL.

 TABLE 3
 CASE CONDITIONS

Case	Condition	Time
Case 1	10 % voltage drop	0.25 s until 0.325 s
Case 2	20° phase jump	0.4 s until 0.475 s
Case 3	0.8 Hz frequency jump	0.55 s until 0.625 s
Case 4	harmonic distortion	0.7 s until 0.775 s

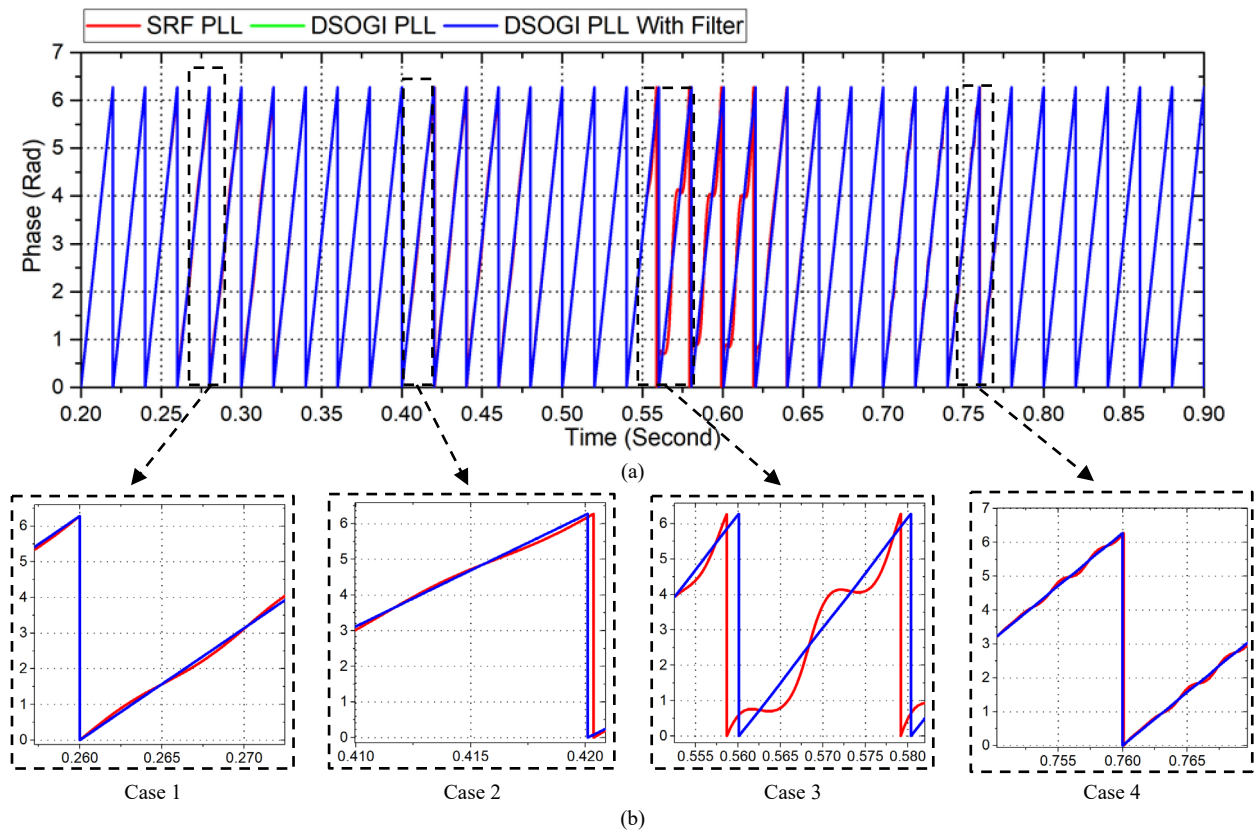


Figure 7. Phase estimation (a) phase estimation of DSOGI PLL with filter, DSOGI PLL, and SRF PLL under several conditions (b) performance phase estimation of DSOGI PLL with filter under several conditions.

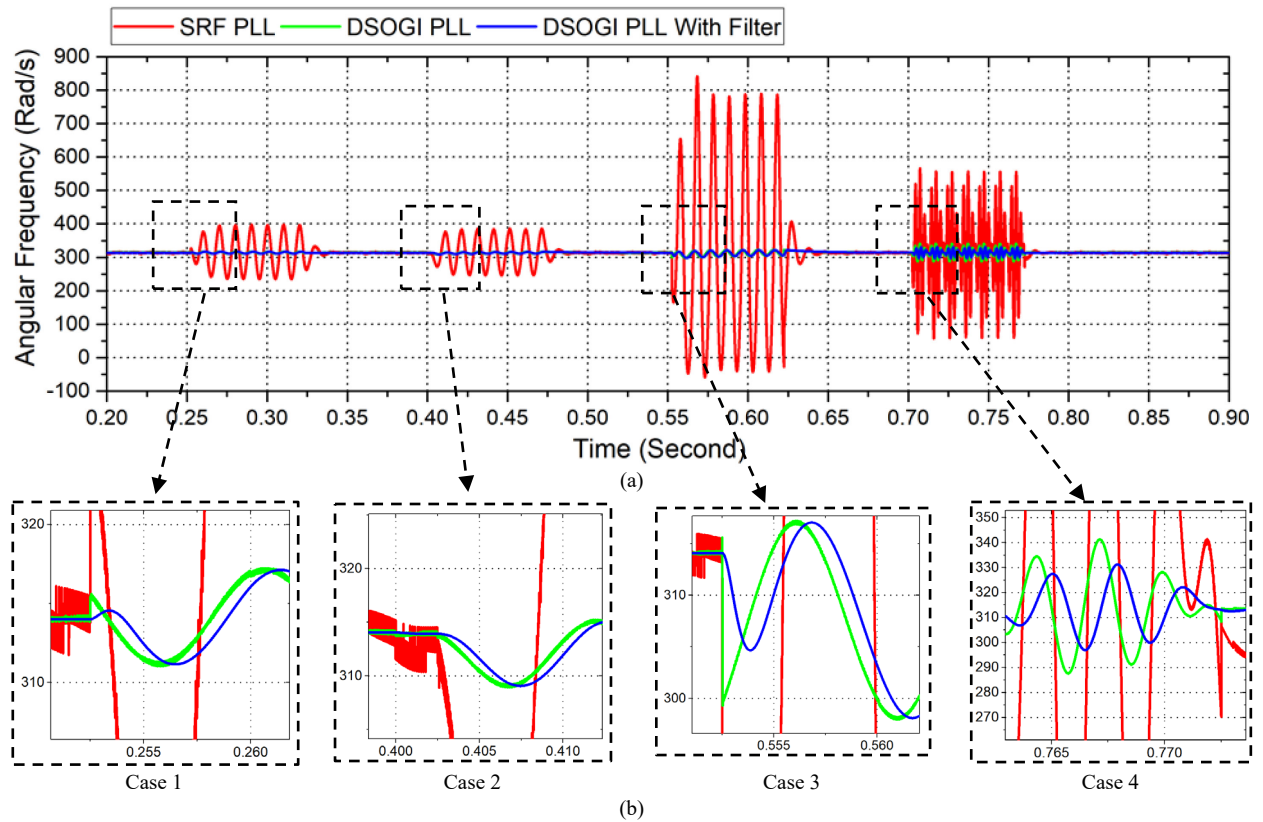


Figure 8. Frequency estimation (a) frequency estimation of DSOGI PLL with filter, DSOGI PLL, and SRF PLL under several conditions (b) performance frequency estimation of DSOGI PLL with filter under several conditions.

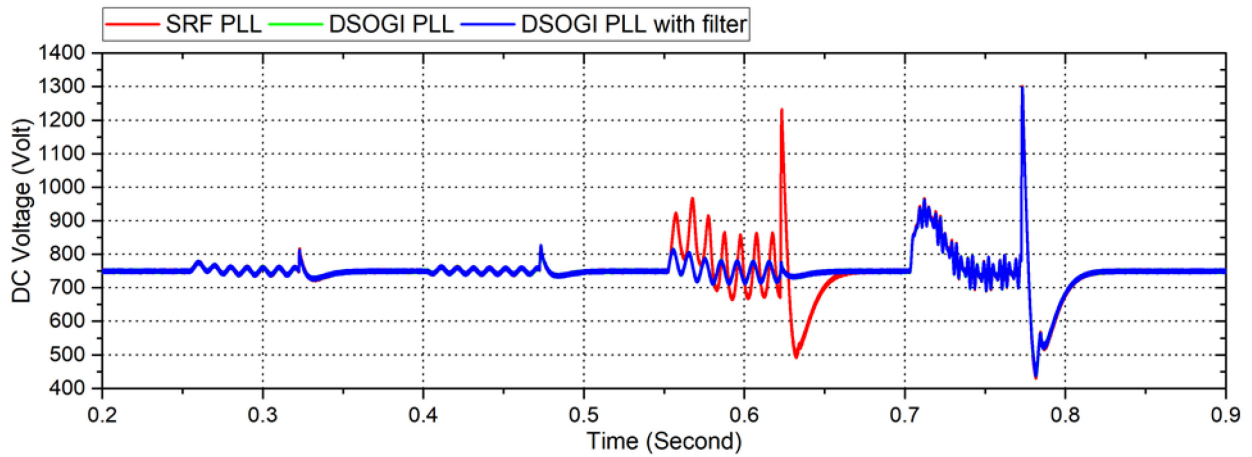


Figure 9. DC voltage condition in several cases using DSOGI PLL with filter, DSOGI PLL, and SRF PLL under several conditions.

 TABLE 4
 THDI ON THE SYSTEM UNDER SEVERAL CONDITIONS

CURRENT		CASE 1			CASE 2			CASE 3			CASE 4		
		PLL (%)	DSOGI PLL (%)	DSOGI PLL with filter (%)	PLL (%)	DSOGI PLL (%)	DSOGI PLL with filter (%)	PLL (%)	DSOGI PLL (%)	DSOGI PLL with filter (%)	PLL (%)	DSOGI PLL (%)	DSOGI PLL with filter (%)
GRID	A	0.1	0.073	0.073	0.18	0.18	0.19	0.52	0.12	0.12	0.34	0.33	0.33
	B	0.16	0.14	0.14	0.26	0.25	0.25	0.34	0.1	0.1	0.35	0.35	0.35
	C	0.22	0.18	0.18	0.12	0.09	0.09	0.78	0.062	0.062	0.61	0.61	0.61
PHASE	A	0.1	0.073	0.073	0.17	0.18	0.19	0.52	0.12	0.12	0.34	0.33	0.33
	B	0.6	0.14	0.14	0.26	0.24	0.25	0.34	0.106	0.1	0.35	0.35	0.35
	C	0.22	0.18	0.18	0.12	0.09	0.09	0.78	0.06	0.06	0.61	0.61	0.61

Figure 7 (a) shows the phase estimation under several cases to evaluate the performance of DSOGI PLL with filter. See Figure 7 (b), the DSOGI PLL with filter can estimate the phase accurately under various conditions. The Performance of DSOGI PLL with filter is similar to the performance of DSOGI PLL under various conditions, while the performance of SRF PLL is the worst especially in case 3.

Figure 8 (a) shows the frequency estimation of DSOGI PLL with filter under several cases. Figure 8 (b) explains that the estimated frequency of DSOGI PLL with filter under case 1 is able to minimize ripples and oscillations. The frequency estimation from DSOGI PLL under case 1 on that condition has an undershoot,

and the DSOGI PLL experiences oscillation as well as DSOGI PLL with filter. Under case 2 DSOGI PLL has the same performance with DSOGI PLL with filter by oscillation. Under case 3, DSOGI PLL has overshoot and undershoot at the beginning, and during case 3 DSOGI PLL has the same oscillations as DSOGI PLL with filter. Under case 4, the performance of DSOGI PLL with filter has a bigger oscillation, similar to the performance of DSOGI PLL with filter. Under case 4, SRF PLL has a bigger oscillation than DSOGI PLL and DSOGI PLL with filter. The biggest oscillation is experienced by SRF PLL in case 3.

 TABLE 5
 THDI UNDER LINEAR AND NON-LINEAR LOAD

CURRENT		LINEAR LOAD			NON-LINEAR LOAD		
		PLL (%)	DSOGI PLL (%)	DSOGI PLL with filter (%)	PLL (%)	DSOGI PLL (%)	DSOGI PLL with filter (%)
GRID	A	0.095	0.095	0.095	0.72	0.72	0.72
	B	0.11	0.11	0.12	0.84	0.84	0.84
	C	0.15	0.15	0.15	3.2	3.2	3.2
PHASE	A	0.12	0.12	0.28	0.58	0.58	0.58
	B	0.09	0.09	0.09	0.25	0.25	0.25
	C	0.043	0.043	0.043	0.48	0.48	0.45
LOAD	A	0.74	0.74	0.74	0.55	0.55	0.55
	B	0.33	0.33	0.33	0.36	0.36	0.36
	C	0.56	0.56	0.56	0.8	0.8	0.8

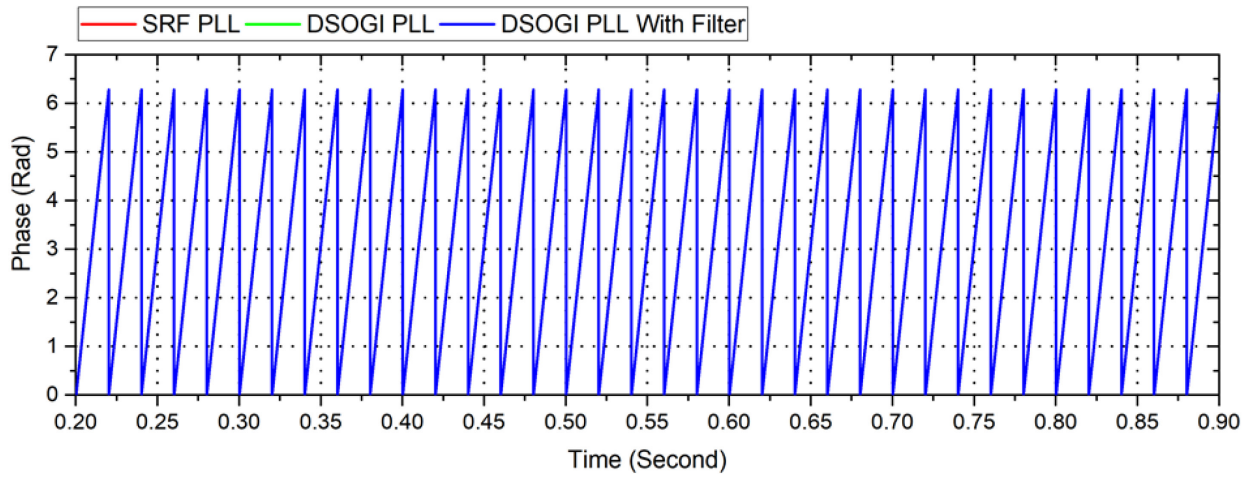


Figure 10. Phase estimation of DSOGI PLL with filter, DSOGI PLL, and SRF PLL under linear and non-linear load.

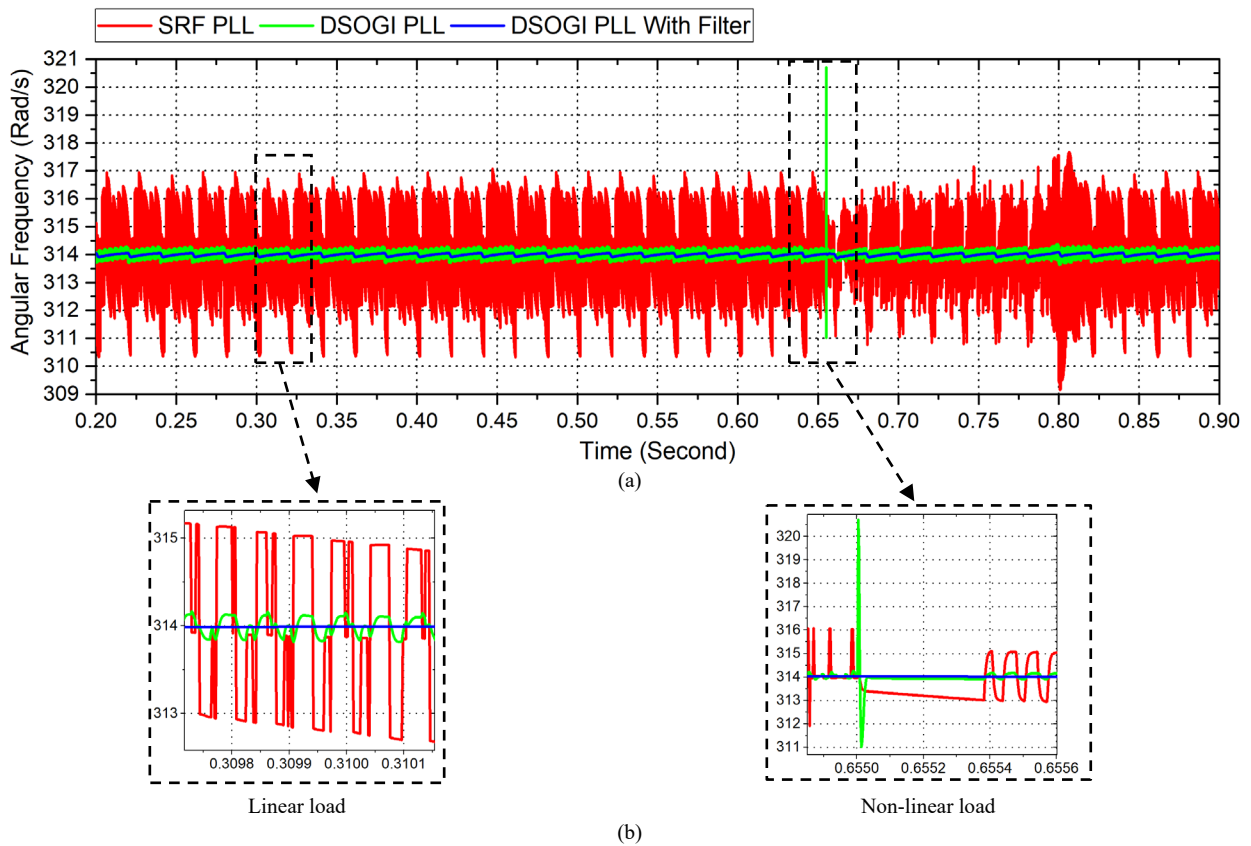


Figure 11. Frequency estimation (a) frequency estimation of DSOGI PLL with filter, DSOGI PLL, and SRF PLL under linear and non-linear load.

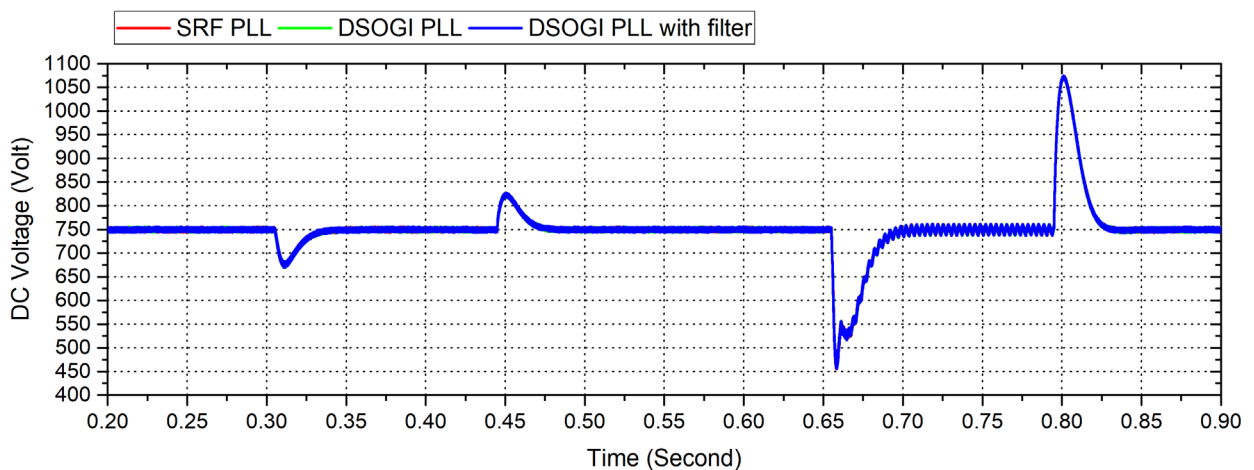


Figure 12. DC voltage of DSOGI PLL with filter, DSOGI PLL, and SRF PLL under linear and non-linear load.

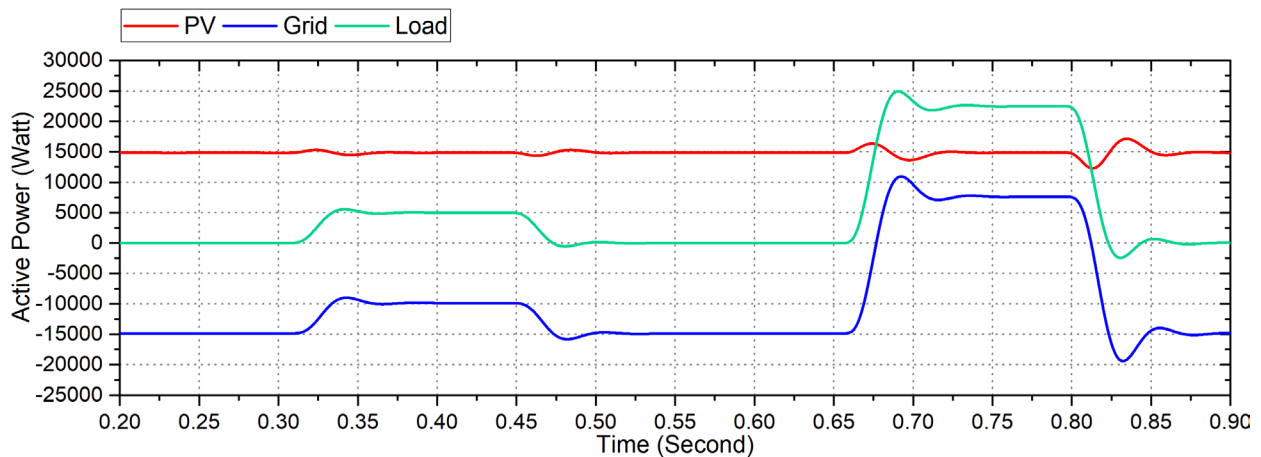


Figure 13. Power flow condition under linear and non-linear load using DSOGI PLL with filter.

Figure 9 shows DC voltage on the performance of DSOGI PLL with filter, DC DSOGI PLL, and SRF PLL. Under case 1 and 2, the comparison shows that the performance of DSOGI PLL with filter is consistent on DC voltage reference at 750 volts with minimum oscillations. This performance is similar to the performance of DSOGI PLL and SRF PLL. Under case 3, the DSOGI PLL with filter has same performance as DSOGI PLL by minimum oscillation. The performance of SRF PLL under case 3 has a bigger oscillation compared with DSOGI PLL and DSOGI PLL with filter. Under case 4, the performance of all algorithm is equal to the oscillation and the large harmonic.

Table 4 shows the comparison between THDi on the system under several conditions when using DSOGI PLL with filter and DSOGI PLL and SRF PLL. The comparison shows that all of them have the same level of THDi and are still in the range from 0.06% to 0.78%. Which is still lower than 5% (IEEE standard 1547(TM)-2003).

The performance of DSOGI PLL with filter is evaluated on linear load and non-linear load to show the power flow of the system. The specification on linear load is 5kW and the specification of the non-linear load is three-phase inverter 22.5kW.

Table 5 shows that THDi on the system under linear and non-linear load using DSOGI PLL with filter is compared with DSOGI PLL and SRF PLL. The comparison shows that all of them has the same level of THDi and still in the range from 0.043% to 3.2%. The biggest THDi occurs in non-linear load conditions because the non-linear load is a harmonic source. This level of THDi is smaller than IEEE standard 1547(TM)-2003 (5%).

Figure 10 shows the comparison of phase estimation using DSOGI PLL with filter, DSOGI PLL, and SRF PLL. The comparison shows that the phase estimation of DSOGI PLL with filter, DSOGI PLL, and SRF PLL are the same. The harmonic distortion generated from non-linear load can't affect the phase estimation.

Figure 11 (a) shows the frequency estimation of DSOGI PLL with filter under linear and non-linear load. The comparison shows DSOGI PLL with filter is accurate to estimate the frequency. DSOGI PLL with

filter can be precisely at 314 Rad/s angular frequency but DSOGI PLL has a minimum oscillation, while SRF PLL has a bigger oscillation. Figure 11 (b) shows that there is no impact from the linear load on frequency estimation, where frequency estimation is precise on 314 Rad/s. On the non-linear load, DSOGI PLL with filter is precise on 314 Rad/s, while DSOGI PLL in the transience to non-linear load experience overshoots and undershoots, and the frequency estimation during the non-linear load is distorted by ripple. SRF PLL still experiences great oscillation during system running.

Figure 12 shows the comparison of DC voltage of DSOGI PLL with filter, DSOGI PLL, and SRF PLL. The comparison shows that the DC voltage of DSOGI PLL with filter, DSOGI PLL, and SRF PLL are the same. The harmonic distortion generates from non-linear load can't affect the DC voltage.

The power flow using DSOGI PLL with filter and SRF PLL have the same performance. Figure 13 shows the power flow using DSOGI PLL with filter under 5 kW linear load and 22.5 kW non-linear load. It can be seen that the power flow occurs due to different load conditions. Figure 13 shows that the initial load is 5 kW. Therefore, the PV system is capable to supply power to the load. The remaining power 10 kW flows into the grid. When the PV power is not enough to supply power to the 22.5 kW load, the grid supplies the remaining 7.5 kW of power. This means that the PV still supplies 15 kW power to the load. The result of the simulation shows that the PV system is capable to operate during grid-connected and transient condition.

VII. CONCLUSION

In this work, synchronization based on algorithm DSOGI PLL is improved with filter on the grid-connected PV system simulation. The performance of DSOGI PLL with filter is compared to DSOGI PLL and SRF PLL under several conditions. The performance of DSOGI PLL with filter is more efficient to extract phase estimation and frequency estimation of grid voltage under several conditions by minimizing ripples and oscillations. The efficient of DSOGI PLL with filter is shown by minimum oscillations and ripples on frequency estimation, and by a minimum error on phase estimation and error on DC voltage. In the linear load

and non-linear load, the system is capable to supply the power. The harmonic ripples of system fulfill the harmonic standards for PV systems (IEEE standard 1547(TM)-2003). In the future work, we propose a method for tuning PI control in synchronization control to achieve efficiency on the three-phase grid-connected PV system.

ACKNOWLEDGMENT

This work was supported by UNNES Electrical Engineering Students Research Group (UEESRG), Department of Electrical Engineering, Universitas Negeri Semarang.

REFERENCES

- [1] World Energy Council, "World Energy Resources 2016," in *World Energy Resources 2016*, 2016, pp. 1–33.
- [2] J. Khoury, R. Mbayed, G. Salloum, E. Monmasson, and J. Guerrero, "Review on the integration of photovoltaic renewable energy in developing countries - Special attention to the Lebanese case," *Renew. Sustain. Energy Rev.*, vol. 57, pp. 562–575, May 2016.
- [3] IEA PVPS, "Annual Report 2013," 2013.
- [4] Z. Abdmouleh, A. Gastli, L. Ben-Brahim, M. Haouari, and N. A. Al-Emadi, "Review of optimization techniques applied for the integration of distributed generation from renewable energy sources," *Renewable Energy*, vol. 113, pp. 266–280, Dec. 2017.
- [5] D. Boroyevich, I. Cvetkovic, R. Burgos, and D. Dong, "Intergrid: A future electronics energy network?," *IEEE Journal of Emerging Selected. Topics in Power Electronics*, vol. 1, no. 6, pp. 127–136, Sep. 2013.
- [6] K. Arulkumar, K. Palanisamy, and D. Vijayakumar, "Recent Advances and Control Techniques in GridConnected Pv System – A Review," *International Journal of Renewable Energy Research*, vol. 6, no. 3, pp. 1031–1049, 2016.
- [7] H. Calleja and H. Jimenez, "Performance of a grid connected PV system used as active filter," *Energy Conversion and Management*, vol. 45, no. 15–16, pp. 2417–2428, Sep. 2004.
- [8] X. Tang, K. M. Tsang, and W. L. Chan, "Power conditioning system for grid-connected photovoltaic system," *Solar Energy*, vol. 96, pp. 187–193, Oct. 2013.
- [9] S. L. Prakash, A. S. Jesudaiyan, and M. Arutchelvi, "Dynamic Simulation of Grid Tied PV-Inverter Under Distorted Grid Voltage," *International Journal Of Innovative Research In Electrical, Electronics, Instrumentation And Control Engineering*, vol. 2, no. 9, pp. 1926–1932, 2014.
- [10] S. Natesan and J. Venkatesan, "A SRF-PLL control scheme for DVR to achieve grid synchronization and PQ issues mitigation in PV fed grid connected system," *Circuits and Systems*, vol. 07, no. 10, pp. 2996–3015, 2016.
- [11] P. Kanjiya, B. Singh, A. Chandra, and K. A. Haddad, "SRF Theory Revisited" to Control Self Supported Dynamic Voltage Restorer (DVR) for Unbalanced and Nonlinear loads," *IEEE Transactions on Industry Applications*, vol. 49, issue 5, pp. 1-9, 2013.
- [12] F. Blaabjerg, R. Teodorescu, M. Liserre, and A. V. Timbus, "Overview of control and grid synchronization for distributed power generation systems," *IEEE Trans. on Industrial Electronics*, vol. 53, no. 5, pp. 1398–1409, Oct. 2006.
- [13] A. Nicastrì and A. Nagliero, "Comparison and evaluation of the PLL techniques for the design of the grid-connected inverter systems," in *Proc. IEEE International Symposium on Industrial Electronics*, 2010, pp. 3865–3870.
- [14] M. Ciobotaru, R. Teodorescu, and F. Blaabjerg, "A new single-phase PLL structure based on second order generalized integrator," in *Proc. IEEE Power Electronics Specialist Conference*, 2006.
- [15] A. Luna, C. Citro, C. Gavriluta, and J. Hermoso, "Advanced PLL structures for grid synchronization in distributed generation," *Renewable Energy and Power Quality Journal*, pp. 1747–1756, Apr. 2012.
- [16] I. Setiawan, M. Facta, A. Priyadi, and M. H. Purnomo, "Comparison of three popular PLL schemes under balanced and unbalanced grid voltage conditions," in *Proc. 2016 8th International Conference on Information Technology and Electrical Engineering*, 2016, pp. 6–11.
- [17] V. Kaura and V. Blasko, "Operation of a phase locked loop system under distorted utility conditions," *IEEE Trans. on Industry Applications*, vol. 33, no. 1, pp. 58–63, 1997.
- [18] R. Urhekar and S. U. Kulkarni, "Study and simulation of SOGI PLL for single phase grid connected system," *International Journal of Scientific Research in Science, Engineering and Technology*, vol. 2, no. 2, pp. 741–745, 2016.
- [19] H. E. P. de Souza, F. Bradaschia, F. A. S. Neves, M. C. Cavalcanti, G. M. S. Azevedo, and J. P. de Arruda, "A method for extracting the fundamental-frequency positive-sequence voltage vector based on simple mathematical transformations," *IEEE Trans. Ind. Electron.*, vol. 56, no. 5, pp. 1539–1547, May 2009.
- [20] A. Kulkarni and V. John, "A novel design method for SOGI-PLL for minimum settling time and low unit vector distortion," in *Proc. IECON Industrial Electronics Conference*, 2013, pp. 274–279.
- [21] S. Golestan, M. Monfard, F. D. Freijedo, and J. M. Guerrero, "Design and tuning of modified power based PLL for single phase grid connected power conditioning system," *IEEE Trans. on Power Electronics*, vol. 27, no. 8, pp. 3639–3650, Aug. 2012.
- [22] *IEEE Std 1547a-2014 - IEEE Standard for Interconnecting Distributed Resources with Electric Power Systems Amendment 1*, 2014.
- [23] F. Spertino and G. Graditi, "Power conditioning units in grid-connected photovoltaic systems: a comparison with different technologies and wide range of power ratings," *Solar Energy*, vol. 108, pp. 219–229, Oct. 2014.
- [24] B. Singh and F. Ieee, "Power Balance Theory Based Control of Grid Interfaced Solar Photovoltaic Power Generating System with Improved Power Quality," in *Proc. IEEE International Conference on Power Electronics, Drives and Energy System*, 2012.
- [25] A. B. Rey-Bou, R. Garcia-Valverde, F. D. A. Ruz-Vila, and J. M. Torrelo-Ponce, "An integrative approach to the design methodology for 3-phase power conditioners in Photovoltaic Grid-Connected systems," *Energy Conversion and Management*, vol. 56, pp. 80–95, Apr. 2012.
- [26] H. Dammah, I. Lachkar, and S. L. Elhaq, "MPPT and PFC achievement in grid connected photovoltaic system based on a half bridge inverter," in *Proc. International Conference on Control Engineering & Information Technology*, 2016, pp. 16–18.
- [27] A. Haque, "Maximum Power Point Tracking (MPPT) scheme for solar photovoltaic system," *Energy Technolgy & Policy*, vol. 1, no. 1, pp. 115–122, Jan. 2014.
- [28] L. Gao, R. A. Dougal, S. Liu, and A. P. Iotova, "Parallel-connected solar PV system to address partial and rapidly fluctuating shadow conditions," *IEEE Trans. on Industrial Electronics*, vol. 56, no. 5, pp. 1548–1556, May 2009.

- [29] A. Gupta, "Three Phase Inverter Simulation using Sinusoidal PWM Technique," *International Journal of Advanced Research in Electrical, Electronics and Instrumentation Engineering*, vol. 6, issue 5, pp. 4102–4108, May 2017.
- [30] S. Kharjule, "Voltage source inverter," in Proc. *International Conference Energy Systems and Applications*, 2015.
- [31] S. R. Bowes and D. Holliday, "Comparison of pulse-width-modulation control strategies for three-phase inverter systems," in *IEE Proc. Electric Power Applications*, 2006.
- [32] N. Mutoh, M. Ohno, and T. Inoue, "A method for MPPT control while searching for parameters corresponding to weather conditions for PV generation systems," *IEEE Trans. Industrial Electronics*, vol. 53, no. 4, pp. 1055–1065, June 2006.
- [33] S. K. Chung, "A phase tracking system for three phase utility interface inverters," *IEEE Trans. Power Electronics*, vol. 15, no. 3, pp. 431–438, May 2000.
- [34] N. F. Guerrero-Rodríguez, A. B. Rey-Boué, L. C. Herrero-de Lucas, and F. Martínez-Rodrigo, "Control and synchronization algorithms for a grid-connected photovoltaic system under harmonic distortions, frequency variations and unbalances," *Renewable Energy*, vol. 80, pp. 380–395, Aug. 2015.
- [35] P. Rodríguez, R. Teodorescu, I. Candela, A. V. Timbus, M. Liserre, and F. Blaabjerg, "New positive-sequence voltage detector for grid synchronization of power converters under faulty grid conditions," in Proc. of PESC - *IEEE Power Electronics Specialist Conference*, 2006.
- [36] Y. Han, M. Luo, X. Zhao, J. M. Guerrero, and L. Xu, "Comparative performance evaluation of orthogonal-signal-generators-based single-phase PLL algorithms - A Survey," *IEEE Trans. on Power Electronics*, vol. 31, no. 5, pp. 3932–3944, May 2016.
- [37] M. Ciobotaru, R. Teodorescu, and V. G. Agelidis, "Offset rejection for PLL based synchronization in grid-connected converters," in Proc. *IEEE Applied Power Electronics Conference and Exposition - APEC*, 2008, no. 1, pp. 1611–1617.
- [38] *Park, Inverse Park And Clarke, Inverse Clarke Software, Transformations MSS Implementation, Microsemi*, 2013.
- [39] A. Elsebaay, M. Ramadan, M. A. A. Adma, "Studying the Effect of Non-Linear Loads Harmonics on Electric Generator Power Rating Selection," *European Scientific Journal*, vol. 13, no. 18, pp. 1857-7881, July 2017.
- [40] A. P. Singhal, Defferance Between Linear Loads and Non-Linear Loads, *Tricolite website*. [Online] Available: <http://www.tricolite.com/pdf/sources-eEffects-harmonics.pdf>
- [41] N. Kuyvenhoven, "PID Tuning Methods An Automatic PID Tuning Study with MathCad," *Calvin College ENGR. 315*, Dec. 2002.